



A comprehensive theoretical study of thermal relations in plant tissue following electroporation



Samo Mahnič-Kalamiza^{a,b,*}, Nataša Poklar Ulrih^b, Eugène Vorobiev^c, Damijan Miklavčič^a

^aUniversity of Ljubljana, Faculty of Electrical Engineering, Tržaška c. 25, SI-1000 Ljubljana, Slovenia

^bUniversity of Ljubljana, Biotechnical Faculty, Jamnikarjeva 101, SI-1000 Ljubljana, Slovenia

^cSorbonne Universités, Université de Technologie de Compiègne, Laboratoire TIMR, Centre de Recherche de Royallieu, B.P. 20529, 60205 Compiègne Cedex, France

ARTICLE INFO

Article history:

Received 15 November 2016

Received in revised form 16 March 2017

Accepted 17 March 2017

Available online 5 April 2017

Keywords:

Electroporation

Pulsed electric fields

Thermal relations

Mathematical modelling

Heat transfer

LaLoThEq models

ABSTRACT

Electroporation is the application of electric pulses of sufficient amplitude to target tissue, which entails not only permeabilization of cell membranes, but also heat generation and dissipation. Noticeable rises in temperature have been observed in a number of electroporation applications. These temperature rises are a potential source of alteration of thermodynamic properties of tissue wherein mass transport is occurring. Transport parameters are temperature-dependent, as they relate to thermodynamic processes.

This paper presents a theoretical study of thermal relations in tissue immediately following electroporation. An analysis of thermal transfer characteristics of tissue based on available data from literature is performed, and a model of heat transfer in tissue is presented. The tissue is modelled as a porous medium, and the chosen model for analysis, which we call the dual-porosity model, is a two-temperature model developed for heterogeneous porous materials. The dual-porosity model in its given form is a particular example of a LaLoThEq (Lack of Local Thermal Equilibrium) model. This model is used to evaluate the potential for any significant alteration of cell membrane's thermal conductivity due to electroporation, and examines whether electroporation thus directly influences heat redistribution in tissue.

The main result is an in-depth theoretical analysis on the potential influence of electroporation on heat transfer characteristics of tissue via any direct influence of the treatment to the cell membrane. Findings of the study indicate that, on the contrary to the effects of electroporation on mass transport in tissue, the treatment would appear to exert a negligible influence on heat redistribution, at least due to its direct impact on the cell membrane. Other impacts of electroporation that could potentially result in a heterogeneous heat (re)distribution in tissue are briefly discussed, albeit not the subject of this study.

© 2017 Elsevier Ltd. All rights reserved.

1. Introduction

An electric field of sufficient strength can cause an increase of conductivity and permeability of cell membrane. The effect is known as electroporation and is attributed to creation of aqueous pathways in the membrane [40]. Electroporation is essentially the application of electric pulses of sufficient amplitude to cells or target tissue, with the purpose of achieving the permeabilised state of the cell's lipid bilayer membrane.

Quantifying mass transport and heat transfer (both transmembrane and in bulk tissue) in connection with electroporation of biological tissues is an important research objective. The ability to fully comprehend transport processes has ramifications in all applications of electroporation. Understanding mass transport is

* Corresponding author at: University of Ljubljana, Faculty of Electrical Engineering, Laboratory of Biocybernetics, Tržaška c. 25, SI-1000 Ljubljana, Slovenia.

E-mail address: samo.mahnic-kalamiza@fe.uni-lj.si (S. Mahnič-Kalamiza).

particularly important, in example, for improving juice extraction and facilitating selective extraction/introduction of compounds from/into plant cells [27,47], introducing new electroporation-based technologies and medical treatments [14,31], and solving environmental challenges via use of the so-called “green” biorefinery [13,21]. Since heat generation (Joule heating) is unavoidably associated with electroporation, either as an undesired side effect [11] or an effect that is actively exploited in applications of thermal tissue ablation and ohmic heating [17,25,32], it is important to understand heat transfer in electroporation applications as well.

While electroporation continues to be intensively investigated, there is a persisting lack of models that can be used to model heat transfer and mass transport in complex structures such as biological tissues with relation to electroporation at the macro scale. This paper presents an attempt at extending an existing theoretical mathematical description – the “dual-porosity” model – for studying mass transport in electroporated tissue. The model is adapted to the problem of heat transfer in order to elucidate whether the

cell membrane presents a significant barrier to heat transfer in tissue, and to answer the question of whether electroporation alters this barrier, if at all present, through its effect on the membrane.

A model, called the dual-porosity model, was recently adapted for the field of electroporation research [6,29,30] employing mass conservation and transport laws that enables coupling effects of electroporation to the membrane of individual cells with the resulting mass transport (and, by extension through analogy, transmembrane heat transfer and heat transfer in tissue). The model leans strongly upon firmly established approaches presented in previous works that are devoted to similar oft-encountered problems in chemical engineering [15,24]. These approaches in studying mass transport all benefit from a well-known mathematical analogy of heat and mass transfer, and consequently, the developed dual-porosity model is a special case of the classical LaLoThEq (Lack of Local Thermal Equilibrium) model for porous media [35, 39,43,44], which has long been present in literature on heat transfer. An analytical solution has been found for the presented dual-porosity model formulation, however, the model can (and should, through further development) easily be extended with additional dependencies to account for heterogeneities in tissue and temporal component of electroporation, and then solved numerically.

Due to the finite resistance of biological tissue, electroporation unavoidably entails the flow of an electric current through the tissue. This current through, what is electrically an ohmic load, results in heat generation and dissipation. This means that thermal effects are necessarily integrally and inseparably associated with electroporation. Noticeable rises in temperature have been noted in a number of electroporation applications [1,18,19]. These temperature rises are a potential source of alteration of the thermodynamic properties of the material where mass transport is occurring. Parameters such as viscosity, diffusion rate coefficient, and the rate of chemical reactions and changes are known to be strongly dependent on temperature, since they are fundamentally related to thermodynamic processes.

Thermal effects associated with electromagnetic fields are of high importance in biomedical applications, such as electrochemotherapy and tissue ablation by irreversible electroporation [8,9,16,50], gene transfer [23,41], or radiofrequency ablation [49]. In medical treatments, much attention is dedicated to ensuring that the damage to healthy tissue, which would ideally be left unaltered by the treatment, is under control and kept at the lowest possible extent, and various modelling techniques have been employed to evaluate Joule heating and subsequent thermal generation and dissipation. Numerical finite element models are often employed due to the complexity of the system (tissue heterogeneities and anisotropy) and the relatively complex form of the Pennes bioheat equation [36] that is habitually used to describe thermal relations in perfused tissues.

Thermal relations in biological material treated with electromagnetic fields have been studied extensively across a range of applications and on multiple scales by using various approaches, ranging from pure *in silico* molecular dynamics studies and theoretical non-equilibrium thermodynamics models to *in vivo* studies on model animal tissues. An early consideration of the effects of Joule heating associated with electroporation is presented in e.g. [20]. The authors present an account of model development, whereby a theoretical model was developed to estimate the power dissipation in individual cells during electroporation. They concluded that although heating that may be considered as insignificant at the macroscopic level of a cell suspension or tissue, may actually be substantial on the level of the cell membrane. This supposed rise in temperature could be responsible for a lowering of the threshold required for electroporation, as thermal energy is additionally raising the energy level of the bilayer. This has

recently been re-evaluated and examined in a study presenting an analytical model for calculating the cell membrane temperature gradient [12]. The authors of the study show that electric field generates cell membrane temperature gradients, particularly during sequential pulsing over a sustained period of time. They conjecture that thermal gradients may contribute to electroporation through induced transmembrane voltages.

A recent study in molecular dynamics simulations [34] shed more light on the heat conduction characteristics of the cell membrane itself, by studying heat conduction characteristics of a DPPC lipid bilayer. Thermal conductivity of the lipid bilayer that was evaluated in this molecular dynamics simulation was found to be anisotropic, and lower than that of bulk water. This is thought to be mainly due to the lipid composition at the centre of the bilayer, where acyl chains of lipid molecules face each other due to a loss of the covalent-bond and low number density, and thermal conductivity is the lowest. Even lower than thermal conductivity across the bilayer was found to be the thermal conductivity along the bilayer, meaning the bilayer exhibits a strong anisotropic behaviour in terms of heat conduction.

Another field of electroporation applications that has received considerable attention in studying and modelling thermal effects with and without relation to mass transport is skin electroporation, where electric fields are used for breaching the impermeable stratum corneum for topical drug or gene delivery. The reader is referred to Ref. [5] in particular for a thermal study, or [38] for a more comprehensive review. Modelling thermal relations in skin electroporation is a challenging task, mainly due to highly variable properties between various layers of skin [4,37]. A recent study [42] presents the development of a complex analytical bioheat model for studying temperature increases in electroporation of a subcutaneous tumour, accounting for the multi-layer heterogeneous structure of the skin.

Very different considerations and approaches as compared to the field of biomedical applications can be found in the food processing and other industrial applications of electroporation. In these application areas, it is not a rarity to find treatment protocols delivering high energies to target biological material, and high currents that are present in tissues during long treatment times can cause a substantial rise in temperature due to ohmic heating [47]. Ohmic heating using lower voltages for longer periods of time can, with or without electroporation, also be intentionally used as mild treatment of raw material to increase the rate of mass transfer within tissue [25,48]. Modelling with the purpose of studying thermal effects in this field is mainly limited to various models dealing with the generation and distribution of heat in continuous-flow treatment chambers [26,22], with the purpose of optimising their design, thus avoiding hot spots that can otherwise cause electrode material degradation or treatment chamber deterioration. Theoretical studies relating thermal relations in electroporated plant tissue in industrial applications focusing on enhancing mass transport are virtually non-existent, and presently studies mainly comprise phenomenological models relating electrical or thermal damage to tissue with treatment parameters.

The title of this paper title bears no mention of mass transport, however, we wish to emphasize the inseparable connection between electroporation, the thermal effects that are associated with it, and mass transport processes in tissue. The relations between these (all fundamentally thermodynamic) processes are complex and interdependent. Recent research has shown [12] that thermal gradients across the plasma membrane can result in the differences in *electric potential* on either side of the membrane, meaning that there seems to exist a positive feedback connection whereby thermal gradients resulting from electroporation can alter electric relations on the membrane, thus affecting electroporation, heat, and mass transfer directly.

Building upon previous work [28,29,30], this paper gives a complete presentation of the thermal formulation of the dual-porosity LaLoThEq model, analogous to its mass transport formulations, and the applicability of such a model is discussed and theoretically analysed. The model formulation, as given, can be considered sufficiently detailed for studying thermal relations in electroporated plant tissues, but could also conceivably be extended in a suitable way (e.g. by the Pennes bioheat equation) to facilitate evaluation of thermal effects to the post-electroporation mass transport processes in case of perfused animal tissues. The given thermal model could easily be coupled, via the temperature-dependent mass transport parameters, to the previously developed mass transport models of diffusion and liquid flow during pressing, which is a planned future undertaking. The work presented herein related to thermal relations is entirely theoretical in nature, based on existing literature and extension of the work done previously with mass transport modelling. Validation and evaluation of suitability of these formal mathematical formulations is a work in progress and considered out of scope of this research paper.

2. The theoretical basis and the dual-porosity model

2.1. The heat distribution model – basic model equations and its derivation

By analogy of the Fick’s law of diffusion and Darcy’s law for liquid flow, the dual-porosity model of diffusion has been translated to the problem of filtration-consolidation of biological tissue during pressing (compare [29] with [28], or refer to [30]. By a physically and mathematically equivalent analogy with the Fourier law (see Fig. 1), and using basic relations from non-equilibrium thermodynamics, one can postulate that a dual-porosity model can be written (in its original, non-simplified form) also to describe thermal relations in biological tissue, and this should, in principle, be applicable irrespective of whether the tissue is electroporated or not.

The equations of the thermal (i.e. heat transfer) model for the case of thermal flux along one principal axis, for the extracellular and the intracellular space are, respectively

$$(1 - F) \frac{\partial T_e}{\partial t} - (1 - F) \frac{k_e}{\rho C_p} \frac{\partial^2 T_e}{\partial z^2} - \frac{h_v}{\rho C_p} (T_i - T_e) = 0 \tag{1}$$

$$F \frac{\partial T_i}{\partial t} + \frac{h_v}{\rho C_p} (T_i - T_e) = 0 \tag{2}$$

In Eq. (1) and (2), the factors F and $1 - F$ are the intracellular and extracellular fractions of volume, respectively, i.e. they account for the specific relative volume fraction of each space in a block of tissue – F for example is the bulk volume fraction of cells. As tissue normally comprises cells in more than half its volume, we must account for the conservation of energy in the transmembrane flux term. In order to do so, the member representing transmembrane heat exchange in both equations must be equal, as it represents the same thermal flux. Note that temperatures T_e and T_i in all of the equations presented herein are *intrinsic* quantities, that is, they are temperatures that would actually have been measured, had a probe been inserted to measure the temperature at a given point or into an infinitesimally small volume anywhere in either the extra- or intracellular space. If one, however, measures the bulk temperature in a given finite fraction of volume ΔV of tissue, which occurs in practice, the measured temperature will be, theoretically, a volume-averaged sum of the two respective space contributions. It is therefore important to distinguish between the bulk temperatures (volume-averaged) and their intrinsic definitions [33]. Note that Eq. (2) is missing the diffusive term that would represent the intracellular heat conduction, i.e. the second derivative of temperature on spatial coordinate. This is due to the particular spatial configuration of the system; the intracellular space is not continuous, therefore, heat must traverse the membrane in order to be transferred along the spatial coordinate due to the (supposed) thermal gradient. If both spaces were continuous, both equations would feature the diffusive term, and would be mathematically equivalent.

Dividing Eq. (1) by $1 - F$ and Eq. (2) by F , one obtains

$$\frac{\partial T_e}{\partial t} - \frac{k_e}{\rho C_p} \frac{\partial^2 T_e}{\partial z^2} - \frac{h_v f_v}{\rho C_p F} (T_i - T_e) = 0 \tag{3}$$

Analogous fundamental phenomenological laws



Henry Darcy and the Darcy’s law of fluid flow through a porous medium

$$q_z = -\frac{k}{\mu} \frac{\partial p}{\partial z}$$



Joseph Fourier and the Fourier’s law of heat conduction

$$q_z = -\lambda \frac{\partial T}{\partial z}$$



Adolf E. Fick and Fick’s law of diffusion governing diffusion of a gas across a fluid membrane

$$q_z = -D \frac{\partial c}{\partial z}$$

Fig. 1. The three analogous fundamental laws (and the men they are named after, or in their honour) in simplified differential form for gradient in one spatial dimension. The analogous form of the three laws can be successfully exploited to arrive at the three analogous forms of the dual-porosity model. In the featured equations, q is either the fluid, thermal, or solute flux density (i.e. flow per unit area), k is the coefficient of hydraulic conductivity, D is the solute diffusion coefficient, λ is the material’s heat conductivity coefficient, T is local temperature, c denotes local concentration, p is local liquid pressure, while z is the spatial coordinate.

$$\frac{\partial T_i}{\partial t} + \frac{h_v}{\rho c_p F} (T_i - T_e) = 0 \quad (4)$$

In Eq. (3), the new parameter – the volumetric fraction ratio f_v – is a multiplicative factor accounting for the volumetric space distribution imbalance and equalling $F/(1-F)$. Other quantities are as follows: T_e and T_i are the extracellular and the intracellular temperature in K, respectively; k_e is the extracellular tissue thermal conductivity in $\text{W m}^{-1} \text{K}^{-1}$; z (in m) is the spatial and t (in s) the temporal coordinate; c_p is the tissue heat capacity in $\text{J kg}^{-1} \text{K}^{-1}$; ρ the tissue density in kg m^{-3} ; and h_v the volumetric heat transfer coefficient in $\text{W m}^{-3} \text{K}^{-1}$. Coefficient h_v reflects the thermal conductivity of the plasma membrane and the particular heat exchange geometry, and a spatio-temporal dependence of the parameter as a function of electroporation can at this point be postulated to maintain complete generality. Whether such a dependence exists or not remains to be theoretically and experimentally evaluated, which is the main aim of this study. Section 2.3 is largely devoted to this question. Note that the fraction f_v/F in Eq. (3) that equals $(1-F)^{-1}$ has intentionally not been resolved for purposes of simplifying the following algebra. Instead, we define a volume fraction-normalized volumetric heat transfer coefficient h'_v , which equals $h'_v = h_v/F$.

Reviewing previous work on the dual-porosity model of mass transport [30], a comparison would reveal that models are mathematically analogous, with concentration or liquid pressure gradients now replaced by thermal gradients. There is an important difference however, stemming from the values of the transport parameters. In the thermal problem, the thermal conductivities, if comparing those of cytoplasm, plasma membrane, and extracellular liquid, are found not to differ from each other by orders of magnitude (see [12,34]). With mass or liquid transfer on the other hand, the permeability of the cell membrane was modelled as orders of magnitude lower than that of either the intra- or the extracellular space. In the latter case, the finite diffusion velocity in the intracellular space, not captured by the model, could be safely neglected. In the thermal model on the other hand, thermal resistances are within the same order of magnitude, to which some additional careful consideration has to be given (see Section 2.3).

The system of Eq. (3) and (4) can be readily solved by using analytical methods given appropriate initial and boundary conditions (see Section 2.2). If studying the distribution of temperature within tissue after electroporation or ohmic heating, one can suppose that the tissue sample has been heated to a given temperature T_0 both

in the extra- and the intracellular space (i.e. $T_0 = T_{e0} = T_{i0}$), and that during subsequent treatment, if no additional heat is generated, all surfaces of the sample are exposed to the ambient temperature T_{amb} , where $T_{\text{amb}} < T_0$ (cooling). In mathematical notation, and taking the symmetry on either side of the plane at $z = 0$ perpendicular to the principal axis of thermal flux into account (analogous to the diffusion problem – see [29]), one can write

$$T_e|_{z=h/2} = T_{\text{amb}} \quad (5)$$

$$\left. \frac{\partial T_e}{\partial z} \right|_{z=0} = 0 \quad (6)$$

$$T_e|_{t=0} = T_i|_{t=0} = T_0 \quad (7)$$

where the plane of symmetry ($z = 0$) is located exactly in the middle of the tissue sample of height h at a distance of $h/2$ from either of the sample's largest surfaces, at which the bulk of heat exchange is taking place (see Fig. 2). Note that since Eq. (1) (or Eq. (3) for that matter) is missing any spatial derivatives, it is in fact an ordinary differential equation for T_i and requires no boundary conditions. The actual intracellular temperature at the boundaries is therefore determined entirely by the values of the extracellular temperature at these boundaries.

The set of Eqs. (3)–(7) represents a complete mathematical description of thermal dissipation out of the sample block of tissue. The contribution of electroporation to the thermal conductivity of the membrane, if substantial, can be accounted for by varying the transmembrane volumetric heat transfer coefficient h_v , and in case of additional thermal generation (time of observation during the electroporation application), an additional additive member accounting for heat generation can be appended to both Eqs. (3) and (4). The system of equations could conceivably even be extended to take the form of the Pennes bioheat equation in case of studying perfused animal tissues. Anisotropy can be modelled via a spatial dependence of k_e , and a similar approach can be used for the heat capacity and/or density, if required. The resulting augmented model can then easily be solved via numerical integration; however, the main problem (as with the other two analogous models, i.e. the dual-porosity diffusion and liquid expression models) remains the (un)reliable parameter estimation for realistic systems and the high number of degrees of freedom that the large number of parameters introduces to the model.

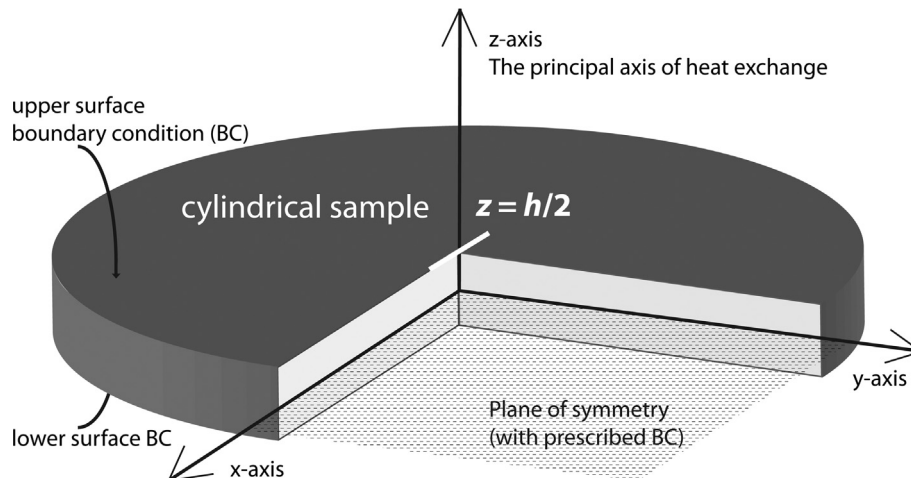


Fig. 2. The thermal problem geometry – plane of symmetry and boundary conditions. The particular cylindrical geometry of the tissue sample is not significant, but has been used for this illustration for purposes of maintaining consistency with mass transport studies. For the presented schematic to be an adequate representation of the actual state, the sample and setup geometry has to favour thermal transfer along only one (principal) axis.

2.2. The thermal dual-porosity model – analytical solution

The system of Eqs. (3) and (4) with boundary and initial conditions Eqs. (5)–(7) is essentially an integro-differential system admitting various methods for obtaining an analytical solution.

Using the method of separation of variables – which the reader is most likely familiar with and therefore the details of the procedure are omitted from the following text – it is possible to obtain an analytical solution for the intra- and extracellular temperature profiles in space and time.

One can begin by first rewriting partial differential equations of the system into a suitable form, thus

$$\frac{\partial T_e}{\partial t} = \frac{k_e}{\rho c_p} \frac{\partial^2 T_e}{\partial z^2} + \frac{f_v h'_v}{\rho c_p} (T_i - T_e) \tag{8}$$

$$\frac{\partial T_i}{\partial t} = -\frac{h'_v}{\rho c_p} (T_i - T_e) \tag{9}$$

To simplify the arithmetic in the following presentation of the solution, new constants α and β can be introduced, where $\alpha = k_e/\rho c_p$ and $\beta = h'_v/\rho c_p$, and thus

$$\frac{\partial T_e}{\partial t} = \alpha \frac{\partial^2 T_e}{\partial z^2} + f_v \beta (T_i - T_e) \tag{10}$$

$$\frac{\partial T_i}{\partial t} = -\beta (T_i - T_e) \tag{11}$$

The purpose of introducing h'_v should now be obvious from Eqs. (10) and (11) above. In order to further simplify calculations and presentation of results, it is convenient to introduce new variables to observe only temperature differences in relation to the ambient temperature instead of working with absolute values, thus

$$T_{e,\delta} = T_e - T_{amb} \tag{12}$$

$$T_{i,\delta} = T_i - T_{amb} \tag{13}$$

This necessitates some corrections to the boundary conditions, which now read

$$T_{e,\delta}|_{z=h/2} = T_{amb} - T_{amb} = 0 \tag{14}$$

$$\left. \frac{\partial T_{e,\delta}}{\partial z} \right|_{z=0} = 0 \tag{15}$$

and initial conditions are henceforth equal to the temperature differences between the absolute and ambient temperature,

$$T_{e,\delta}|_{t=0} = T_e|_{t=0} - T_{amb} = T_{e0,\delta} \tag{16}$$

$$T_{i,\delta}|_{t=0} = T_i|_{t=0} - T_{amb} = T_{i0,\delta} \tag{17}$$

In continuation, the introduced δ -notation is kept throughout for clarity and as a reminder; the reader should beware that both T_e and T_i were redefined by Eqs. (12) and (13), and these equations should be consulted in order to obtain absolute values of temperature from their ‘ δ ’ counterparts. The use of temperature differences also requires that particular attention be paid in case the modelled process involves phase transitions whose effects are not accounted for by the present model.

To solve the system 10–11, the classical method of separation of variables can be used [7] as previously mentioned. Taking the orthogonal Fourier series of functions (that one arrives at after separating the variables and taking boundary conditions into the account) of the form

$$\Theta(z, t) = \frac{4}{\pi} \sum_{n=0}^{\infty} \frac{(-1)^n}{2n+1} C_n \cos(\lambda_n z) e^{-\lambda_n^2 \alpha t} \tag{18}$$

where $\lambda_n = (2n + 1)\pi/l$, l is the full thickness of the tissue sample, the final step is to account for the initial condition by varying the remaining undetermined coefficients C_n for both the intra- and the extracellular space. After completion of this procedure, one arrives at the final form of the particular solution of the system 3–4, which is

$$T_{e,\delta}(z, t) = \frac{4T_{i0,\delta}}{\pi} \sum_{n=0}^{\infty} \frac{(-1)^n}{2n+1} \times \cos(\lambda_n z) \left[C_{n,1} e^{\gamma_{n,1} t} \left(\frac{\gamma_{n,1}}{\beta} + 1 \right) + C_{n,2} e^{\gamma_{n,2} t} \left(\frac{\gamma_{n,2}}{\beta} + 1 \right) \right] \tag{19}$$

$$T_{i,\delta}(z, t) = \frac{4T_{i0,\delta}}{\pi} \sum_{n=0}^{\infty} \frac{(-1)^n}{2n+1} \times \cos(\lambda_n z) [C_{n,1} e^{\gamma_{n,1} t} + C_{n,2} e^{\gamma_{n,2} t} - e^{-\beta t}] + T_{i0,\delta} e^{-\beta t} \tag{20}$$

where

$$C_{n,1} = \frac{\left(\frac{T_{e0,\delta}}{T_{i0,\delta}} - 1 \right) \beta - \gamma_{n,2}}{\gamma_{n,1} - \gamma_{n,2}} \tag{21}$$

$$C_{n,2} = \frac{\left(1 - \frac{T_{e0,\delta}}{T_{i0,\delta}} \right) \beta + \gamma_{n,1}}{\gamma_{n,1} - \gamma_{n,2}} \tag{22}$$

and where

$$\gamma_{n,2} = \frac{-((f_v + 1)\beta + \lambda_n^2 \alpha) \pm \sqrt{((f_v + 1)\beta + \lambda_n^2 \alpha)^2 - 4\lambda_n^2 \alpha \beta}}{2} \tag{23}$$

The eigenvalues λ_n equal $\lambda_n = (2n + 1)\pi/l$.

This analytical solution is instructive. It indicates that the process kinetics is determined entirely by the roots of the characteristic polynomial (given by Eq. (23)). Additionally, were the transmembrane volumetric heat transfer coefficient h'_v equal to 0, i.e. if the cell membrane would have thermally isolative properties, Eq. (19) would simplify into the better known classical one-dimensional heat conduction equation

$$T_{e,\delta}(z, t) = \frac{4T_{0,\delta}}{\pi} \sum_{n=0}^{\infty} \frac{(-1)^n}{2n+1} e^{-\left(\frac{(2n+1)^2 \pi^2 \alpha t}{l^2} \right)} \cos(\lambda_n z) \tag{24}$$

In the opposite case of the infinitely conductive cell membrane, the same conclusion can be drawn, albeit this may not be immediately obvious from the solution Eqs. (19)–(23). Letting $\beta \rightarrow \infty$ would consequentially always result in the difference $T_{i,\delta} - T_{e,\delta}$ equalling zero, i.e. a temperature gradient across the cell membrane would be impossible to establish. In this case, the last additive member (the source term) in Eqs. (10) and (11) is always zero, i.e. the two spaces are perpetually in complete local thermal equilibrium (LoThEq), and there is no lack of local thermal equilibrium that would justify the use of the dual-porosity model. Given this observation and the previously established approximate equality of the intra-, the extracellular, and the membrane thermal conductivities, one could already suppose that the membrane will not present an obstacle to thermal conduction between the cells and in tissue. For completeness and in order to corroborate this finding by sounder theoretical analysis, transport parameters such as the volumetric transmembrane heat transfer coefficient h'_v should be evaluated first, in order to definitively establish whether the membrane presents a barrier to heat transfer or not.

To illustrate the spatio-temporal distribution of temperature in a hypothetical situation of tissue cooling after being heated to different temperatures intra- and extracellularly, Fig. 3 gives thermal profiles in the extracellular space for several different values of the

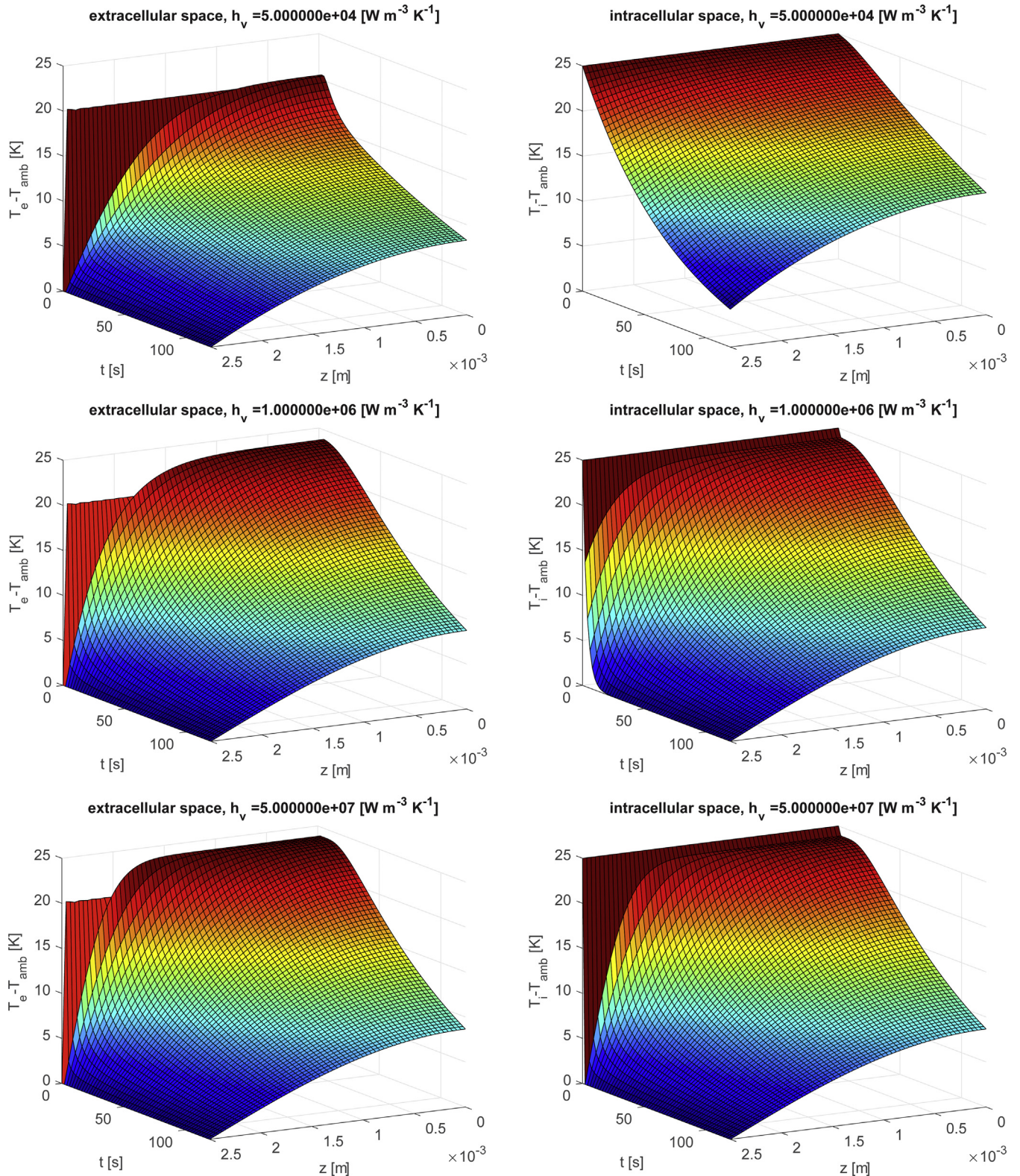


Fig. 3. The spatio-temporal profiles of the intrinsic temperature in the intra- and extracellular space for three different values of the transmembrane volumetric heat transfer coefficient h_v . The initial temperatures (relative difference from T_{amb}) were $T_{i0,s} = 25\text{ }^\circ\text{C}$ and $T_{e0,s} = 20\text{ }^\circ\text{C}$ in all cases. The first two thousand members of the Fourier cosine series ($n = 0 \dots 1999$) were taken in Eqs. (19) and (20) to ensure the artefacts originating from the discontinuity at $z = l/2$ between the initial and the boundary condition are not visible in the surface plots (stability of the solution).

transmembrane volumetric heat transfer coefficient h'_v . To facilitate an easier comparison by display of simulated results, Fig. 3 presents a plot of $T_{i,s}(z = 0, t)$ and $T_{e,s}(z = 0, t)$ for different values of h'_v . The presented curves are intrinsic temperature kinetics (time

profiles) taken from the centre of the tissue sample where temperature is the highest. Parameters that were used to obtain these simulated model results with the analytical solution are collected in Table 1 (with references). This illustrative situation may not

Table 1
Parameters used in simulations presented in this section.

Parameter	Value	Source	Parameter	Value	Source
l (m)	0.005	Previous experiments [30]	ρ (kg m ⁻³)	1000	Water [45]
F (-)	0.80	Arbitrarily chosen	c_p (J kg ⁻¹ K ⁻¹)	4200	Water [2,45]
k_e (W m ⁻¹ K ⁻¹)	0.559	Apple juice [2]	h'_v (W m ⁻³ K ⁻¹)	varied	n/a
t_{end} (s)	120	Arbitrarily chosen	$T_{i0,\delta}$ (K)	25	arb. chosen
f_v (-)	4	$F/(1-F)$	$T_{e0,\delta}$ (K)	20	arb. chosen

be entirely hypothetical. Tissue composition is heterogeneous in general, and intracellular space may contain more water than extracellular, where there is perhaps a larger volume fraction of air (e.g. apple fruit tissue). Under such conditions of heterogeneity, thermal properties are different between the two spaces as well, which could conceivably lead to two different rates of heat generation and accumulation in the two spaces. Moreover, due to differences in composition, not only thermal but also electrical properties of the spaces are not equal, providing a further possible cause of heterogeneous heat generation.

Fig. 4 gives is a better presentation of the thermal relations in the two spaces immediately after the start of the simulated heat dissipation for five different values of the transmembrane volumetric heat transfer coefficient and up to 60 s of the simulated experiment.

As is shown in Figs. 3 and 4, higher values of the volumetric heat transfer coefficient h'_v permit heat transfer from the intracellular space into the extracellular due to the hypothetical initial difference of 5 °C between the two spaces. This difference in temperatures is purely hypothetical, and its value was chosen arbitrarily for demonstrative purposes. It could conceivably come about due to differing rates of heat generation in the extra- and the intracellular space. Regardless of whether its origin is realistic or whether it is purely hypothetical in nature, the purpose of this initial difference is to demonstrate the transmembrane heat transfer kinetics for varied values of h'_v , as shown in Figs. 3 and 4. Fig. 4 shows that heat transfer can be almost instantaneous (from the point of view of the simulation length, which is 2 min) for very high values of h'_v , or it can be delayed if h'_v is not very large. See Section 2.3 for a discussion on realistic values of this parameter in biological tissues (apple model study). Note that due to the rather large volume fraction of 0.8 used for these simulated kinetics, the heat transfer from the intracellular to the extracellular space does not result in a large

reduction of the intracellular temperature, however, it does result in a proportionally large increase in the extracellular temperature, where f_v is the proportionality factor (conservation of energy!).

The value of k_e representing the extracellular thermal conductivity is that of apple juice, taken as a first approximation, and will be revisited and revised in Section 2.3. All other parameters were chosen to simulate a possible experimental situation with tissue, except of volume fraction F that was slightly reduced (from about 0.92 found in apples to 0.80) in order not to amplify the effect of parameter f_v in Figs. 3 and 4 too extensively. The initial temperatures were chosen arbitrarily for demonstrative purposes and are not important in terms of kinetics, since the model is linear and the final result can thus be scaled.

As a final note to this section, consider that in the eventual presence of a transmembrane thermal gradient, i.e. a difference between the intracellular and the extracellular temperature (in case the transmembrane heat exchange would be noticeably hindered – see Section 2.3 for a discussion), the bulk tissue temperature as measured in a finite volume ΔV comprising cells and extracellular space would, in relation to the intrinsic quantities worked with herein, equal

$$(T_{\text{bulk},\delta})_{\Delta V} = [(1-F)T_{e,\delta} + FT_{i,\delta}]_{\Delta V} \quad (25)$$

2.3. A theoretical estimation of the volumetric heat transfer coefficient h'_v and other parameters; a discussion on the relevance of the dual-porosity model for the thermal problem in electroporated tissues

The parameter h'_v , called the volumetric heat transfer coefficient, relates the temperature difference across the interface (e.g. a membrane) separating the continuous phase (e.g. extracellular space) and the discontinuous phase (e.g. intracellular space), with the resulting local heat generation or dissipation in the respective

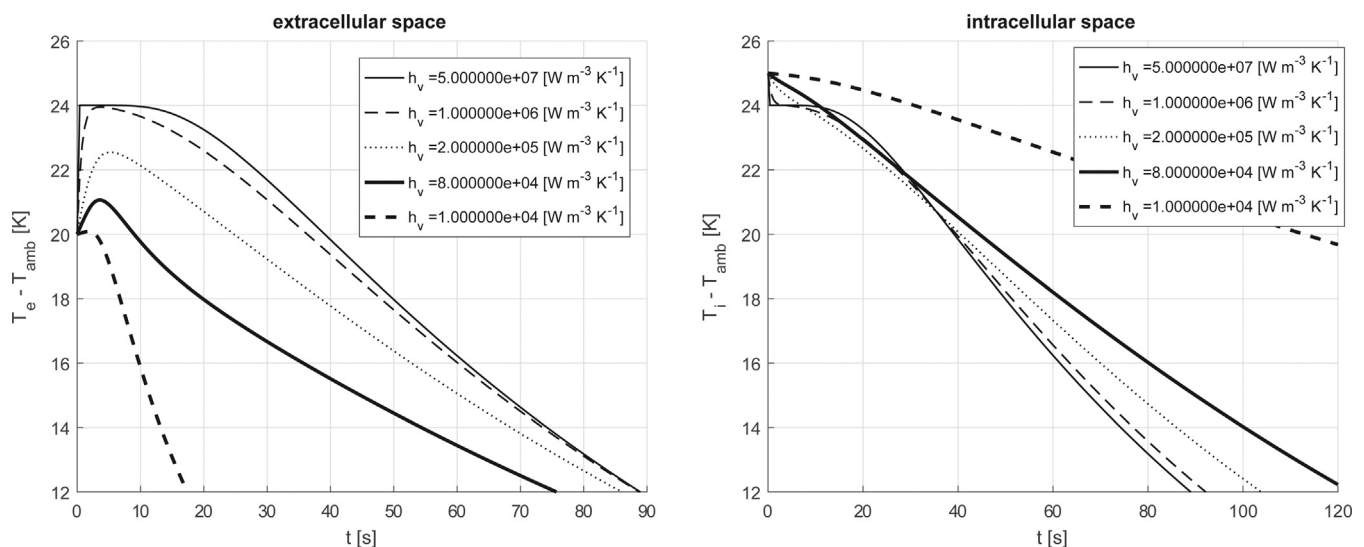


Fig. 4. The kinetics at $z = 0$ (sample centre plane) of the intrinsic temperature in the intra- and extracellular space for five different values of the transmembrane volumetric heat transfer coefficient h'_v .

phases or spaces. Given the medium density and specific heat capacity, this causes a local increase or decrease in temperature, as described by Eqs. (3) and (4).

To arrive at an estimate for h_v in the particular case of biological tissue comprising cells with biological membranes, the following two paths leading to the same conclusion can be taken. Note that the following analysis does not concern itself with h'_v , since the relation between h_v and h'_v is trivial, as it is a matter of a simple linear dependence on the cell volume fraction F .

First, consider the Fourier law of thermal conduction in its differential form with thermal transfer occurring only along one spatial dimension. Writing for the membrane (index m) and in a spherical coordinate system, it reads

$$\dot{q}_m = -k_m \frac{dT}{dr} \quad (26)$$

Integrating across the membrane where the heat flux density q_m is non-zero and the temperature changes from intracellular $T_{i,m}$ to the extracellular $T_{e,m}$ in the immediate proximity to the membrane (denoted by index m), yields

$$\dot{q}_m \int_R^{R+d_m} dr = -k_m \int_{T_{i,m}}^{T_{e,m}} dT \quad (27)$$

Resolving the integrals results in

$$\dot{q}_m = \frac{k_m(T_{i,m} - T_{e,m})}{d_m} \quad (28)$$

where d_m is the membrane thickness (about 4–5 nm).

The expressed heat flux density is in W m^{-2} , and the source term in the dual-porosity model fundamental equations is in W m^{-3} . It is necessary thus to express the heat flux per unit volume, q_v , and the expression involves the particular problem geometry

$$\dot{q}_v = a_v \dot{q}_m = a_v h(T_{i,m} - T_{e,m}) = h_v(T_{i,m} - T_{e,m}) \quad (29)$$

where h is the heat transfer coefficient in $\text{W m}^{-2} \text{K}^{-1}$, h_v the volumetric heat transfer coefficient in $\text{W m}^{-3} \text{K}$, and a_v the surface-to-volume ratio reflecting the particular geometry. In case of spherical cells of radius R , this coefficient equals

$$a_v = \frac{A_c}{V_c} = \frac{4\pi R^2}{\frac{4\pi R^3}{3}} = \frac{3}{R} \quad (30)$$

and therefore

$$\dot{q}_v = a_v \dot{q}_m = \frac{3k_m(T_{i,m} - T_{e,m})}{d_m R} = h_v(T_{i,m} - T_{e,m}) \quad (31)$$

from where it immediately follows

$$h_v = \frac{3k_m}{d_m R} \quad (32)$$

Second, consider the Fourier law of thermal conduction in the differential form, but written for the amount of heat transferred across the membrane per unit time Q_m , not for flux q_m

$$\dot{Q}_m = -k_m 4\pi r^2 \frac{dT}{dr} \quad (33)$$

Separating the variables left/right-hand side and integrating as before, yields, after some rearrangement

$$\begin{aligned} \dot{Q}_m &= \frac{4\pi k_m(T_{i,m} - T_{e,m})}{\frac{1}{R} - \frac{1}{R+d_m}} = \frac{4\pi k_m(T_{i,m} - T_{e,m})}{\frac{d_m}{R(R+d_m)}} \\ &= \frac{4\pi R(R+d_m)k_m(T_{i,m} - T_{e,m})}{d_m} \end{aligned} \quad (34)$$

For $R \gg d_m$, which is valid for biological cells under consideration, one can take the approximation $R + d_m \approx R$ and the Eq. (34) simplifies to

$$\dot{Q}_m = \frac{4\pi R^2 k_m(T_{i,m} - T_{e,m})}{d_m} \quad (35)$$

The simplification step $R + d_m \approx R$ also exists in the first approach that was presented above, however, it is implicit and hidden in Eq. (30), or more precisely, already in Eq. (29). For R approximately equal or on the same order of magnitude as d_m , a more complex expression than Eq. (30) must be used. A discussion on this can be found in previous work, see for example Eq. (A.7) of Appendix A in [28].

Expressing the amount of heat transferred across the membrane Q_m per unit volume, a division with the cell volume V_c is needed to arrive at

$$\dot{q}_v = \frac{\dot{Q}_m}{V_c} = \frac{4\pi R^2 k_m(T_{i,m} - T_{e,m})}{\frac{4\pi R^3}{3}} = \frac{3k_m(T_{i,m} - T_{e,m})}{d_m R} = h_v(T_{i,m} - T_{e,m}) \quad (36)$$

which is exactly the same result as in Eq. (31) and h_v is again equal to exactly the same expression as has already been defined by Eq. (32).

Given a known estimate on the cell size and membrane thickness, the parameter missing in order to obtain h_v is only the transmembrane thermal conductivity, k_m . Since the biological cell membrane is composed of a lipid bilayer, it is expected that its thermal conductivity will be lower than that of cytoplasm and certainly lower than that of bulk water. Molecular dynamics simulations can be used to arrive at an estimate for k_m . In example, authors of [34] report the thermal resistance of the water-lipid bilayer-water system of thickness 40 Å to be $9.3 \cdot 10^{-9} \text{ m}^2 \text{ K W}^{-1}$. Since the thermal resistance equals

$$R_t = \frac{x}{k} \quad (37)$$

where x is the thickness of the resistive layer, k can be recovered from Eq. (37), and for the reported thermal resistance value of $9.3 \cdot 10^{-9} \text{ m}^2 \text{ K W}^{-1}$, k_m is estimated to equal $0.430 \text{ W m}^{-1} \text{ K}^{-1}$. This is about 71% of the thermal conductivity of bulk water, the latter indeed being higher, as was supposed.

For the volumetric heat transfer coefficient of a biological cell of radius 100 μm (e.g. apple fruit cells) and membrane thickness of 5 nm, this k_m yields an h_v according to the following equation,

$$h_v = \frac{3k_m}{d_m R} = \frac{3 \cdot 0.430}{5 \cdot 10^{-9} \cdot 100 \cdot 10^{-6}} = 2.58 \cdot 10^{12} \frac{\text{W}}{\text{m}^3 \text{K}} \quad (38)$$

The value thus obtained is extremely high, however, and this is to be expected. The entire cell area is available for thermal exchange, as opposed to the opposite seen in the mass transfer problems, where only a small fraction on the order of about 10^{-7} – 10^{-4} of the cell membrane area (known as the pore surface fraction – f_p) was available for diffusion or liquid flow. Regardless of this consideration, the volumetric heat transfer coefficient is still unrealistically high, since it has been derived for an idealised system of cytosol-membrane-extracellular space, where the finite thermal resistances of the intracellular and extracellular media do not play any significant role. This was a valid assumption in case of mass transport across a permeabilised membrane [28,29,30], since there, the membrane was the single most important component of the system greatly hindering the transport of mass between the two spaces. In the thermal problem, the thermal conductivity of the membrane is within the same order of magnitude as that of bulk water and thus the cytoplasm, probably also of the extracellular space (of which thermal conductivity will be evalu-

ated in continuation). Moreover, the thickness of the plasma membrane is several orders of magnitude (3–4) lower than is the overall dimension of the cell (the cell radius).

Before the finite thermal conductivity of the cell membrane and its influence are discarded as unimportant, a more realistic estimate of h_v can be obtained and re-evaluated in relation to the intra- and extracellular thermal conductivities and its influence simulated using the dual-porosity model. Only then should any final conclusions be drawn.

Given a finite thermal conductivity/resistance of both the intra- and the extracellular space, the amount of heat transferred across the membrane will be much lower than what would be calculated according to Eq. (35). This equation would hold in the particular case where the membrane's thermal resistance would be so high as to render the finite conductivities on either side of the membrane apparently infinite. This can be further illustrated by noting an apparent absence of any thermal gradients on either side of the membrane, which would mean that $T_i = T_{i,m}$ and $T_e = T_{e,m}$ everywhere in tissue, a situation schematically presented in Fig. 5-left, where the temperature profile at the plasma membrane is drawn in idealised conditions where $k_m \ll k_i$ and $k_m \ll k_e$. A more realistic situation ($k_m \approx k_i \approx k_e$) is illustrated by Fig. 5-right.

The amount of heat transferred across the membrane per unit time is, considering that $k_m \approx k_i \approx k_e$,

$$\dot{Q}_m = \frac{A_c(T_i - T_e)}{\left(\frac{1}{h_i} + \frac{d_m}{k_m} + \frac{1}{h_e}\right)} \quad (39)$$

since thermal resistances are additive. In Eq. (39), $1/h_i$ is the intracellular and $1/h_e$ the extracellular thermal resistance. Following a similar logic as employed during the derivation of the membrane heat transfer coefficient k , one can estimate that h_i equals approximately k_i/R , where R is the radius of an average cell in tissue, and k_i the intracellular thermal conductivity. It is difficult to arrive similarly at a theoretical estimate for h_e , but as a first approximation, it can be considered equal to the intracellular, in particular in systems where $k_i \approx k_e$, which should be a reasonable assumption in first approximation for biological tissues (this will be re-examined in continuation). This logic results in

$$\dot{Q}_m = \frac{A_c(T_i - T_e)}{\left(2\frac{R}{k_i} + \frac{d_m}{k_m}\right)} \cong \frac{A_c k_i (T_i - T_e)}{2R} \quad (40)$$

which is an approximation, since for $k_m \approx k_i$ the term d_m/k_m is insignificant in comparison to R/k_i . From Eq. (40), it is evident that the influence of the membrane on the transmembrane transport has completely vanished from the heat flow estimate, and according to

the assumptions made, the transmembrane heat transfer rate will be governed by the intra- and/or extracellular thermal conductivity (depending on which of these is lower) and the geometric relations of the system, and not by the membrane.

Dividing \dot{Q}_m with the volume of a cell gives the new heat flux per unit volume

$$\dot{q}_m = \frac{\dot{Q}_m}{V_c} = \frac{A_c k_i (T_i - T_e)}{2RV_c} = \frac{3k_i(T_i - T_e)}{2R^2} \quad (41)$$

and the new volumetric heat transfer coefficient equals

$$h_v = \frac{3k_i}{2R^2} = \frac{3 \cdot 0.559}{2(100 \cdot 10^{-6})^2} = 8.385 \cdot 10^7 \frac{W}{m^3 K} \quad (42)$$

which is more realistic, however, still greater than the largest value used in simulations using the analytical solution (see Figs. 3 and 4). The conclusion that can be drawn from this, based on the observed behaviour of the temperatures in Fig. 4 for values of h_v greater than 10^6 , is that any cross-membrane thermal gradient that would result from inhomogeneities in local electric field or current distribution, would be instantaneously (i.e. on a sub-second timescale) annihilated due to the rapid heat transfer across the membrane, as already stipulated by Kotnik and Miklavčič [20].

This finding could potentially lead to the conclusion that the dual-porosity thermal model is unnecessarily complicated with the addition of the source term. This is, however, arguably not the case, since the mathematical analysis is instructive, and the theoretical derivations presented herein can be used to further advance the state of the art of the mass transport analogues of the dual-porosity model. Moreover, the model does allow for the thermal conductivities intra- and extracellularly to differ, and might still be relevant for studying thermal relations in tissue, whether electroporated or not, if the thermal conductivities on either side of the membrane differ significantly. The extremely fast transmembrane thermal transfer does, however, mean that the model is of limited use in studying tissue under conditions of thermal non-equilibrium, since intra-to-extracellular thermal gradients are difficult to establish on the timescale of observation (i.e. seconds to minutes). In other words, as initial differences in temperature cannot come into existence (and so $T_{i0} = T_{e0}$ for all t), there is a constant thermal equilibrium between the spaces resulting in exactly equal thermal kinetics in both spaces, according to simulation.

In order to evaluate whether the general principles of the dual-porosity model as presented can still be useful, in particular for studying heat conduction through bulk tissue, the remainder of

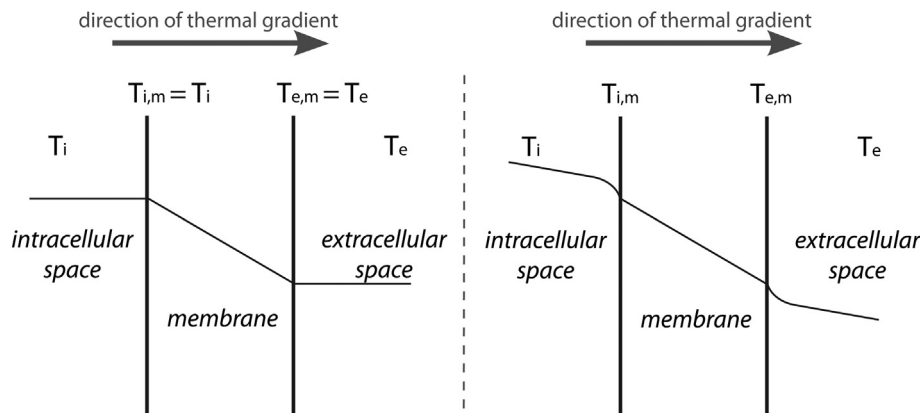


Fig. 5. A schematic illustration of the thermal situation near the membrane for the idealised situation (left) and a more realistic situation reflecting the influence of finite thermal conductivities of the spaces on either side of the membrane (right).

this section is dedicated to a case study of thermal relations in apple tissue. A major part is concerned with determining the intra- and extracellular thermal conductivities, as these parameters must necessarily differ for the model to be applicable. A simulation of an apple tissue sample cooling process then follows this parameter determination.

In cases where there is a marked difference in the thermal properties of the two spaces, i.e. in cases where $k_i \neq k_e$, using the dual-porosity model remains a possibility. Since it has been determined by the preceding analysis that the membrane is too thin to present a significant barrier to heat transfer, it is possible to attribute to the membrane the thermal conductivity of the intracellular space instead, provided $k_i \neq k_e$. By doing so, one supposes that within each individual cell the heat distribution is homogeneous, while heat traverses each cell according to the velocity determined by k_i . This happens to be exactly what is already reflected by Eq. (42), where the transmembrane volumetric heat transfer coefficient no longer depends on any other property of the membrane, but exclusively on the intracellular thermal conductivity.

For apple tissue, tabulated data can be found in literature [2], giving the bulk tissue thermal conductivity at room temperature of about $0.418 \text{ W m}^{-1} \text{ K}^{-1}$, and that of apple juice is $0.559 \text{ W m}^{-1} \text{ K}^{-1}$ (note that this value was used as a first approximation for k_e in the preceding section). There is no reliable data in literature on estimates for the extracellular thermal conductivity. However, using a model of bulk properties of equivalent media such as follow from the modified Maxwell's equivalent medium theory [10], one can suppose that the unknown thermal conductivity (the extracellular) can be obtained from the known bulk thermal conductivity and the supposedly known thermal conductivity of the intracellular space. This is possible assuming that the latter comprises primarily intracellular juice that can be extracted from the cells and its thermal conductivity was independently measured. The extracellular thermal conductivity in apples is presumably much lower than that of the cells, since the juice thermal conductivity is relatively high as compared to apple tissue bulk conductivity. Note that at a higher than 0.5 fraction of cell volume (about 0.92 in apples, see e.g. [30]), according to the equivalent medium model, the extracellular thermal conductivity must be considerably lower to result in a difference of $0.141 \text{ W m}^{-1} \text{ K}^{-1}$ (25% relative to juice) between the bulk and juice thermal conductivities.

The equivalent medium model for a packed bed of spherical particles constituting the *discontinuous* phase embedded in a matrix (i.e. the *continuous* phase) states [2] that

$$k = k_c \frac{1 - [1 - a(k_d/k_c)]b}{1 + (a - 1)b} \quad (43)$$

where k is the bulk thermal conductivity, k_c the thermal conductivity of the continuous and k_d that of the discontinuous phase, b equals $V_d/(V_c + V_d)$ where V_d and V_c are the volume shares of the discontinuous and the continuous phase, respectively, and a equals $3k_c/(2k_c + k_d)$. Cells in tissue (modelled as perfect spheres) form the discontinuous phase, while the extracellular space is the continuous phase in Eq. (43). Setting $k = 0.418 \text{ W m}^{-1} \text{ K}^{-1}$, $k_d = 0.559 -$

$\text{W m}^{-1} \text{ K}^{-1}$, $V_d = 0.92$, and $V_c = 0.08$, the unknown that can be expressed from Eq. (43) is k_e , which is determined by the following expression (the expression following from Eq. (43) for k_e is a quadratic function, of its two roots, only the one yielding a positive k_e is meaningful)

$$k_e = -\frac{2k + bk - k_d - 2bk_d + \sqrt{8(b-1)^2kk_d + ((b+2)k - (2b+1)k_d)^2}}{4(b-1)} \quad (44)$$

with the solution, in our example, $k_e = k_c = 0.174 \text{ W m}^{-1} \text{ K}^{-1}$, which is indeed much lower than either the bulk k or k_d (i.e. k_i). Thus calculated value of k_e is still however almost an order of magnitude greater than thermal conductivity of air, which is (at 20°C and 1 atm) $0.0257 \text{ W m}^{-1} \text{ K}^{-1}$ [45]. This is expected, since in intact apple fruit tissue the extracellular space comprises, besides the extracellular matrix structure, also pockets of air [46], the presence of which is trivially demonstrated by observing that apple fruit tends to float rather than sink in water. The extracellular air, however, is not homogeneously distributed throughout the continuous phase, and is therefore assumed to not be predominantly determining its thermal conductivity.

Table 2 below summarizes all the necessary data allowing for the simulation using the dual-porosity model to be performed out and presented. The results (spatio-temporal distribution of temperature) for the two spaces (i.e. intra- and extracellular space) are given in Fig. 6.

The hypothetical theoretical experiment (simulation), results of which are given in Fig. 6, represents a simulation whereby an apple fruit sample of 5 mm thickness and much larger in the other two dimensions (to assure that the bulk of the thermal flow is only along one axis) is heated (by the electric current during electroporation or otherwise) to 20°C above ambient temperature and then left to rapidly cool (via the electrodes at the boundary surfaces, for example). As the given figure illustrates (Fig. 6-left column), there is no detectable difference between the intra- and the extracellular temperature for such high values of h'_v as realistically calculated for apple fruit cells. The theoretical simulated cell would have to be about 20-times larger (see Fig. 6-right column) in order for a considerable reduction in the transmembrane volumetric thermal conductivity coefficient. This confirms our initial evaluation and the order-of-magnitude analysis of h'_v , which already indicated that the high thermal conductivity of the membrane prevents the appearance of significant transmembrane thermal gradients.

All of the preceding theoretical analysis and simulations using realistic model tissue seem to indicate that there are no noticeable influences of the plasma membrane to the heat transfer in tissue *directly* as a result of the membrane's intrinsic thermal permeability. The membrane is simply too thin and the cells too small for the membrane to present a significant thermal insulation boundary between the intra- and the extracellular space. Therefore, electroporation and its effects to the membrane can be safely assumed to have no *direct* consequences to heat (re)distribution in tissue, at least not on the timescale of seconds or minutes following electro-

Table 2
Parameters used in simulations presented in this section and in some of the theoretical derivations.

Parameter	Value	Source	Parameter	Value	Source
l (m)	0.005	Previous experiments	ρ (kg m^{-3})	1000	Water [45]
F (-)	0.92	Previous works (see [30])	c_p ($\text{J kg}^{-1} \text{K}^{-1}$)	4200	Water [2,45]
k_i ($\text{W m}^{-1} \text{K}^{-1}$)	0.559	Apple juice [2]	k_m ($\text{W m}^{-1} \text{K}^{-1}$)	0.430	[34]
k_e ($\text{W m}^{-1} \text{K}^{-1}$)	0.174	Estimated based on [2]	h'_v ($\text{W m}^{-3} \text{K}^{-1}$)	$8.385 \cdot 10^7$	n/a
t_{end} (s)	120	Arbitrarily chosen	$T_{i0,\delta}$ (K)	20	arb. chosen
f_v (-)	11.5	$F/(1-F)$	$T_{e0,\delta}$ (K)	20	arb. chosen
R (μm)	100	Previous works (see [30])	d_m (nm)	5	[30]

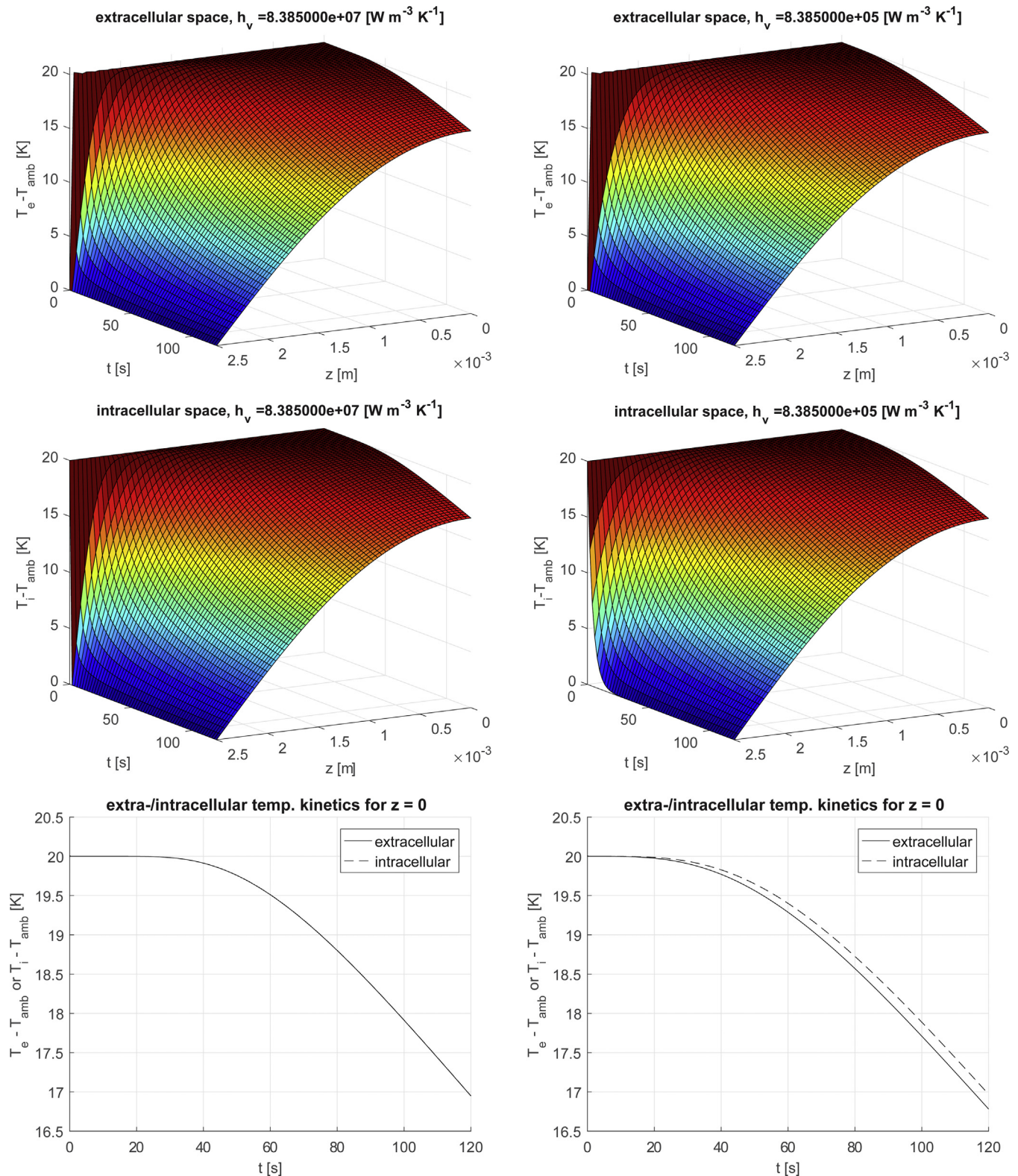


Fig. 6. The results of the dual-porosity model simulation study using the parameters as given in Table 2. Left column: The volumetric heat transfer coefficient was equal to value given in Table 2 (realistic). Right column: The volumetric heat transfer coefficient was reduced by a factor of 100, corresponding to cells 10-times as large as an average apple fruit cell (intentionally exaggerated and unrealistic for demonstration purposes).

poration. However, there still might be undetected effects at the nanometre scale in terms of space and on the micro- to milliseconds timescale during pulse application, a situation which the present study does not explore, as it is limited to the study of thermal

phenomena *after* the application of pulses. Given the emerging use of nano- or even picosecond pulses in electroporation [3], a similar theoretical study into thermodynamics at the membrane would present a welcome elucidation of the problem at the very short

timescale. Such a study however requires a different approach to the one presented herein, and if considered, will be presented separately from the present work.

On the other hand, looking at possible *indirect* consequences of cell membrane electroporation to heat transport in tissue, one cannot neglect the impact of electroporation to redistribution of intercellular juice and consequent changes in local tissue electrical as well as thermal conductivity. If the cell membrane is permeabilised, and liquid vacates the cells (perhaps spontaneously due to release of turgor pressure), this will affect the extracellular electrical and thermal conductivity. This effect will be most pronounced in tissues where the intra- and extracellular conductivities of intact tissue differ the most. For purposes of illustration, consider the extracellular space to comprise pockets of air. These air pockets are poor electrical as well as poor thermal conductors. If, at the onset of electroporation, the air can be replaced with (supplanted by) intracellular juice, this will alter the extracellular space composition and its thermal as well as electrical properties. The degree to which this phenomenon occurs and affects the overall bulk tissue thermal and/or electrical conductivity, will supposedly depend on the degree of electroporation of the cell membranes. For highly permeabilised cells in tissue, the supposition $k_e \approx k_i$ may be a valid assumption, however, if the tissue is intact or subjected only to very gentle electrical treatment, one should expect to observe $k_e < k_i$. In this case, the heat transfer through tissue can be modelled using the thermal dual porosity model whose solution is presented in Section 2.2, however, sufficient accuracy for all practical purposes can probably also be achieved by assuming the tissue being homogeneous with regard to heat exchange.

3. Conclusions

This paper presents work performed within the scope of a broader study dedicated to the problem of characterising mass and heat transfer phenomena and their relation in biological tissues, predominantly those of plant origin. The first section is dedicated to the analogy between the dual-porosity models of mass transport and its equivalent thermal formulation, and gives a detailed analysis of the model from its formulation to development of the analytical solution, as well as providing theoretical grounds for estimating all of the required model parameters. This is followed by an example simulation study using apple fruit tissue as model material. First, a way of estimating all of the required parameters based on those available in the literature is presented, followed by a simulation of cooling of an apple fruit sample. This is done for both a realistic membrane thermal conductivity, as well as an unrealistically altered one, illustrating how different the actual fruit (or plant tissue, in general) structure would have to be in order for the membrane to have a significant effect on cooling kinetics.

The conclusion that can be drawn from the analysis of thermal relations in tissue with the use of the dual-porosity thermal model is that, from the heat transfer point of view, tissue (electroporated tissue in particular) is too homogeneous (if electroporated homogeneously, of course) to necessitate the study of its thermal properties with a more complex model of dual porosity. For all common intents and purposes in industrial applications, the thermal properties of the extracellular and the intracellular space can be considered approximately equal. In this case, bulk properties of tissue can be used in a simple local thermal equilibrium model to study heat relations in tissue with adequate accuracy (first-order kinetics).

The same however cannot be said or claimed for very short timescales and events on the nano-scale that were not considered. The dual-porosity model might present an interesting starting point for modelling thermal relations on the level of cells and on

very short timescales, something that has been shown as important not in the seconds after electroporation, but rather during the pulse application.

Possible future directions in model development point towards combining the heat transfer model with a model of mass transport in tissue, since mass transport parameters are known to exhibit strong temperature dependence. The model could also conceivably be extended by accounting for tissue heterogeneity and anisotropy, however, before delving into such levels of detail, the findings of this theoretical analysis must first be corroborated by experimentally obtained data.

Acknowledgements

The Authors wish to acknowledge the financial support of the Slovenian Research Agency (ARRS) through research programmes “Biochemical and biophysical characterization of natural compounds (P4-0121)” and “Electroporation-based technologies and treatments (P2-0249)”. This work was conducted within the scope of the European Associated Laboratory (LEA) entitled “Pulsed Electric Fields Applications in Biology and Medicine” (LEA EBAM).

References

- [1] H. Allali, L. Marchal, E. Vorobiev, Blanching of strawberries by ohmic heating: effects on the kinetics of mass transfer during osmotic dehydration, *Food Bioprocess Technol.* 3 (2010) 406–414.
- [2] American Society of Heating, 2006 ASHRAE Handbook: Refrigeration: SI Edition (ASHRAE), 2006.
- [3] T. Batista Napotnik, M. Reberšek, P.T. Vernier, B. Mali, D. Miklavčič, Effects of high voltage nanosecond electric pulses on eukaryotic cells (in vitro): A systematic review, *Bioelectrochemistry* 110 (2016) 1–12.
- [4] S. Becker, Transport modeling of skin electroporation and the thermal behavior of the stratum corneum, *Int. J. Therm. Sci.* 54 (2012) 48–61.
- [5] S.M. Becker, A.V. Kuznetsov, Local temperature rises influence in vivo electroporation pore development: a numerical stratum corneum lipid phase transition model, *J. Biomech. Eng.* 129 (2007) 712–721.
- [6] B. Boyd, S. Becker, Modeling of in vivo tissue electroporation and cellular uptake enhancement, *IFAC-PapersOnline* 48 (2015) 255–260.
- [7] J. Crank, *The Mathematics of Diffusion*, Oxford University Press, 1979.
- [8] R.V. Davalos, B. Rubinsky, Temperature considerations during irreversible electroporation, *Int. J. Heat Mass Transf.* 51 (2008) 5617–5622.
- [9] R.V. Davalos, B. Rubinsky, L.M. Mir, Theoretical analysis of the thermal effects during in vivo tissue electroporation, *Bioelectrochemistry* 61 (2003) 99–107.
- [10] A. Eucken, Allgemeine Gesetzmäßigkeiten für das Wärmeleitvermögen verschiedener Stoffarten und Aggregatzustände, *Forsch Ing-Wes* 11 (1940) 6–20.
- [11] P.A. Garcia, R.V. Davalos, D. Miklavcic, A numerical investigation of the electric and thermal cell kill distributions in electroporation-based therapies in tissue, *PLoS ONE* 9 (2014) e103083.
- [12] A.L. Garner, M. Deminsky, V.B. Neculaes, V. Chashihin, A. Knizhnik, B. Potapkin, Cell membrane thermal gradients induced by electromagnetic fields, *J. Appl. Phys.* 113 (2013) 214701.
- [13] A. Golberg, M. Sack, J. Teissie, G. Pataro, U. Pliquett, G. Saulis, T. Stefan, D. Miklavcic, E. Vorobiev, W. Frey, Energy-efficient biomass processing with pulsed electric fields for bioeconomy and sustainable development, *Biotechnol. Biofuels* 9 (2016).
- [14] S. Haberl, D. Miklavcic, G. Sersa, W. Frey, B. Rubinsky, Cell membrane electroporation—Part 2: the applications, *IEEE Electr. Insul. Mag.* 29 (2013) 29–37.
- [15] A. Halder, A.K. Datta, R.M. Spanswick, Water transport in cellular tissues during thermal processing, *AIChE J.* 57 (2011) 2574–2588.
- [16] S.K. Hall, E.H. Ooi, S.J. Payne, A mathematical framework for minimally invasive tumor ablation therapies, *Crit. Rev. Biomed. Eng.* 42 (2014) 383–417.
- [17] Hosahalli S. Ramaswamy, Michele Marcotte, Sudhir K. Sastry, Khalid Abdelrahim, *Ohmic Heating in Food Processing*, 2014.
- [18] H. Jaeger, N. Meneses, J. Moritz, D. Knorr, Model for the differentiation of temperature and electric field effects during thermal assisted PEF processing, *J. Food Eng.* 100 (2010) 109–118.
- [19] B. Kos, P. Voigt, D. Miklavcic, M. Moche, Careful treatment planning enables safe ablation of liver tumors adjacent to major blood vessels by percutaneous irreversible electroporation (IRE), *Radiol. Oncol.* 49 (2015) 234–241.
- [20] T. Kotnik, D. Miklavcic, Theoretical evaluation of the distributed power dissipation in biological cells exposed to electric fields, *Bioelectromagnetics* 21 (2000) 385–394.
- [21] T. Kotnik, W. Frey, M. Sack, S. Haberl Meglič, M. Peterka, D. Miklavčič, Electroporation-based applications in biotechnology, *Trends Biotechnol.* 33 (2015).

- [22] J. Krauss, Ö. Ertunç, C. Rauh, A. Delgado, Novel, Multi-Objective Optimization of Pulsed Electric Field Processing for Liquid Food Treatment, in: K. Knoerzer, P. Juliano, P. Roupas, C. Versteeg (Eds.), *Innovative Food Processing Technologies: Advances in Multiphysics Simulation*, Blackwell Publishing Ltd., 2011, pp. 209–231.
- [23] I. Lackovic, R. Magjarevic, D. Miklavcic, Three-dimensional finite-element analysis of joule heating in electrochemotherapy and in vivo gene electrotransfer, *IEEE Trans. Dielectr. Electr. Insul.* 16 (2009) 1338–1347.
- [24] J.L. Lanoiselle, E.I. Vorobyov, J.M. Bouvier, G. Piar, Modeling of solid/liquid expression for cellular materials, *AIChE J.* 42 (1996) 2057–2068.
- [25] N.I. Lebovka, I. Praporscic, S. Ghnimi, E. Vorobiev, Does electroporation occur during the ohmic heating of food?, *J Food Sci.* 70 (2005) E308–E311.
- [26] M. Lindgren, K. Aronsson, S. Galt, T. Ohlsson, Simulation of the temperature increase in pulsed electric field (PEF) continuous flow treatment chambers, *Innovat. Food Sci. Emerg. Technol.* 3 (2002) 233–245.
- [27] D. Liu, N.I. Lebovka, E. Vorobiev, Impact of electric pulse treatment on selective extraction of intracellular compounds from *saccharomyces cerevisiae* yeasts, *Food Bioprocess Technol.* 6 (2013) 576–584.
- [28] S. Mahnič-Kalamiza, E. Vorobiev, Dual-porosity model of liquid extraction by pressing from biological tissue modified by electroporation, *J. Food Eng.* 137 (2014) 76–87.
- [29] S. Mahnič-Kalamiza, D. Miklavčič, E. Vorobiev, Dual-porosity model of solute diffusion in biological tissue modified by electroporation, *Biochim. Biophys. Acta (BBA) – Biomembr.* 1838 (2014) 1950–1966.
- [30] S. Mahnič-Kalamiza, D. Miklavčič, E. Vorobiev, Dual-porosity model of mass transport in electroporated biological tissue: Simulations and experimental work for model validation, *Innovative Food Sci. Emerg. Technol.* 29 (2015) 41–54.
- [31] B. Mali, T. Jarm, M. Snoj, G. Sersa, D. Miklavcic, Antitumor effectiveness of electrochemotherapy: a systematic review and meta-analysis, *Eur. J. Surg. Oncol.* 39 (2013) 4–16.
- [32] S. McDermott, D.A. Gervais, Radiofrequency ablation of liver tumors, *Semin. Intervent. Radiol.* 30 (2013) 49–55.
- [33] F. de Monte, G. Pontrelli, S. Becker, Chapter 3 - drug release in biological tissues, in: S.M. Becker, A.V. Kuznetsov (Eds.), *Transport in Biological Media*, Elsevier, Boston, 2013, pp. 59–118.
- [34] T. Nakano, G. Kikugawa, T. Ohara, A molecular dynamics study on heat conduction characteristics in DPPC lipid bilayer, *J. Chem. Phys.* 133 (2010) 154705.
- [35] D.A. Nield, A note on the modeling of local thermal non-equilibrium in a structured porous medium, *Int. J. Heat Mass Transf.* 45 (2002) 4367–4368.
- [36] J. Okajima, S. Maruyama, H. Takeda, A. Komiya, Dimensionless solutions and general characteristics of bioheat transfer during thermal therapy, *J. Therm. Biol.* 34 (2009) 377–384.
- [37] N. Pavselj, D. Miklavcic, Resistive heating and electropermeabilization of skin tissue during in vivo electroporation: A coupled nonlinear finite element model, *Int. J. Heat Mass Transf.* 54 (2011) 2294–2302.
- [38] U. Pliquett, Mechanistic studies of molecular transdermal transport due to skin electroporation, *Adv. Drug Deliv. Rev.* 35 (1999) 41–60.
- [39] A. Rees, Microscopic modeling of the two-temperature model for conduction in heterogeneous media, *JPM* 13 (2010).
- [40] L. Rems, D. Miklavčič, Tutorial: electroporation of cells in complex materials and tissue, *J. Appl. Phys.* 119 (2016) 201101.
- [41] C. Rosazza, S.H. Meglic, A. Zumbusch, M.-P. Rols, D. Miklavcic, Gene electrotransfer: a mechanistic perspective, *Curr. Gene. Ther.* 16 (2016) 98–129.
- [42] D. Sarkar, A. Haji-Sheikh, A. Jain, Temperature distribution in multi-layer skin tissue in presence of a tumor, *Int. J. Heat Mass Transf.* 91 (2015) 602–610.
- [43] P. Vadasz, Heat conduction in nanofluid suspensions, *J. Heat Transfer* 128 (2005) 465–477.
- [44] P. Vadasz, On the paradox of heat conduction in porous media subject to lack of local thermal equilibrium, *Int. J. Heat Mass Transf.* 50 (2007) 4131–4140.
- [45] N.B. Vargaftik, *Handbook of Thermal Conductivity of Liquids and Gases*, CRC Press, 1993.
- [46] J.F.V. Vincent, Relationship between density and stiffness of apple flesh, *J. Sci. Food Agric.* 47 (1989) 443–462.
- [47] E. Vorobiev, N. Lebovka, Pulsed-electric-fields-induced effects in plant tissues: fundamental aspects and perspectives of applications, in: *Electrotechnologies for Extraction from Food Plants and Biomaterials*, Springer, New York, 2008, pp. 39–81.
- [48] W.-C. Wang, S.K. Sastry, Effects of moderate electrothermal treatments on juice yield from cellular tissue, *Innovative Food Sci. Emerg. Technol.* 3 (2002) 371–377.
- [49] K. Wang, F. Tavakkoli, S. Wang, K. Vafai, Analysis and analytical characterization of bioheat transfer during radiofrequency ablation, *J. Biomech.* 48 (2015) 930–940.
- [50] A. Zupanič, D. Miklavčič, Tissue heating during tumor ablation with irreversible electroporation, *Elektrotehniški Vestnik* 78 (2011) 42–47.